Mapping Therapeutic Response in a Patient with Malignant Glioma

Sean M. Haney, Paul M. Thompson, Timothy F. Cloughesy, Jeffrey R. Alger, Andrew J. Frew, Alejandro Torres-Trejo, John C. Mazziotta, and Arthur W. Toga

Abstract: Short-interval scanning of patients offers a detailed understanding of the natural progression of tumor tissue, as revealed through imaging markers such as contrast enhancement and edema, prior to therapy. Following treatment, short-interval scanning can also provide evidence of attenuation of growth rates. We present a longitudinal imaging study of a patient with *glioblastoma multiforme* (GBM) scanned 15 times in 104 days on a 3 T MR scanner. Images were analyzed independently by two automated algorithms capable of creating detailed maps of tumor changes as well as volumetric analysis. The algorithms, a nearest-neighbor-based tissue segmentation and a surface-modeling algorithm, tracked the patient's response to temozolomide, showing an attenuation of growth. The need for surrogate imaging end-points, of which growth rates are an example, is discussed. Further, the strengths of these algorithms, the insight gained by short-interval scanning, and the need for a better understanding of imaging markers are also described. **Index Terms:** Glioma—Algorithms—Brain, tumors—Magnetic resonance imaging.

Malignancies of the CNS account for 1% of all human cancers (1). Nonetheless, these malignancies have an enormous impact on the individuals affected by them and their families. Despite extensive research efforts, the prognosis for patients with *glioblastoma multiforme* (GBM) remains dismal. Reported median survival is <1 year (2).

Researchers traditionally have investigated the disease's effect on normal tissue in a "snap-shot" fashion utilizing imaging as macroscopy, histopathology as tissue morphology, and molecular biology to define mechanisms. Malignant gliomas have been well characterized with regard to imaging and histopathology. These tumors are beginning to be better characterized through molecular biology, especially with advent of high throughput systems for analyzing tissue genetics. Attempts have been made to integrate these fields as each one advances over the years, with limited success. Ideally, dynamic integration of these fields would provide a clearer characterization of the biologic processes involving tumor and the surrounding normal tissue. This improved characterization will not only help in investigating the basic tissue and molecular mechanisms but will also lead to improved monitoring of these changes in patients and better monitoring of their reaction to treatment.

The broader goal of this work is to improve analysis of tumor progression and therapeutic response. Tracking a patient's response to therapy through short-interval scanning and growth rate alteration is the specific means of doing so.

One way toward a better understanding of CNS tumors as they appear through MRI is correlating imaging markers with tumor histopathology. This may be accomplished through alignment of postmortem tissue with premortem MR scans. This has already been accomplished in Alzheimer disease (AD), where an AD atlas couples MRI to histopathology, thus providing a powerful tool for researchers with potential applications in diagnosis and evaluation of therapy efficacy (3,4). Tissue correlation may also be accomplished through MR guidance of biopsy and subsequent correlation of features to imaging markers; this method may be used to adjust therapy as well.

In the future, to further advance our understanding of tumor imaging, it may be necessary to apply multimodality analysis. Evaluating T1-weighted postcontrast, T2-weighted, apparent diffusion coefficient, proton density, and MR spectroscopy (MRS) data may prove effec-

tive in dissecting information on underlying tumor biology and provide markers that single modality imaging cannot do. Computer algorithms that maintain stereotaxic space are ideally suited to do so, as imaging data from multiple sources can be interpreted and correlated in a common 3D coordinate system. Stereotaxic space allows for the development of volumetric maps. Applied across the scan interval, volumetric maps can be used to derive maps tracking rates of change in contrast-enhancing tumor tissue, for instance. Maps illustrating growth rates and changes in these rates may be derived and may function as new imaging markers. Growth rates, determined through volumetric analysis of contrast-enhancing tissue across time, for example, can predict response as well as survival (5). As part of this study, we track the attenuation in growth of contrast-enhancing tissue following the addition of temozolomide to a patient's therapy regimen.

Imaging modalities such as MRS and PET are valuable tools in their own right and as complements to MRI and tissue maps derived from them. MRS and PET provide information on the physiology and metabolic activity of tissues and are therefore more tissue specific than MRI. MRS and PET, however, require additional time to acquire, have poorer resolution, and provide none of the information on subtle focal changes that MRI does. In addition, volumetric PET studies usually cannot be performed longitudinally owing to radiation exposure. Rather than simply providing volumetric information, tissue and surface maps capture the boundary geometry of the tumor in 3D and allow the direct mapping of focal or regional change in the stereotaxic space. This approach, in conjunction with other mapping approaches, allows for targeted biopsy and resection, correlation or segmentation of other modality data, and the definition of profiles of particularly aggressive growth.

The long-term goal of the longitudinal study of malignant gliomas, of which this study is part, is to further our understanding of imaging markers, how these markers respond to therapy, and better define the tumor proper in imaging data. The specific goal of this study is, through short-interval scanning, to track dynamic changes in contrast-enhancing tumor tissue in a patient with GBM, thereby gaining greater insight into the response of imaging markers to therapy.
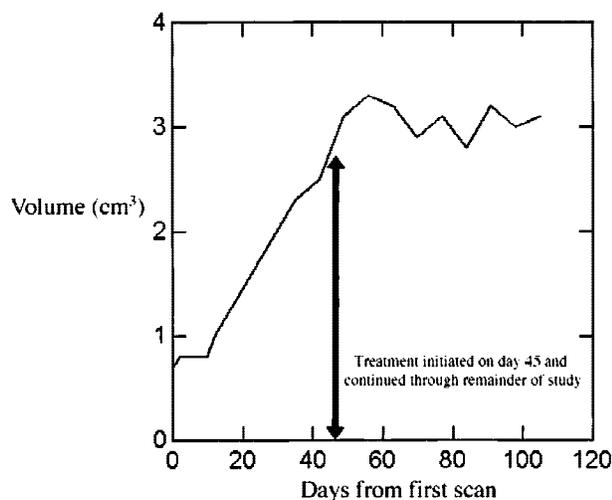
METHODS AND CLINICAL BACKGROUND

Clinical Background

The patient participating in this study, a 59-year-old man, presented with seizures. A contrast-enhancing lesion was observed on CT and MR in the right temporal lobe. The patient underwent a gross total resection. The lesion was categorized as a GBM with oligodendroglioma components by a neuropathologist. The patient subsequently received regional radiation therapy and adjuvant chemotherapy, which included Accutane 100 mg/m^2/day × 21days, with 7 days off. During this 9-month period, the patient was judged on three separate occasions by a neuroradiologist to have stable disease based on MRI. A new lesion was identified approximately a year after the presentation of symptoms. The patient underwent a fluorodeoxyglucose (FDG) PET study. It was not possible, based on FDG-PET, to determine whether the enhancement represented tumor or radiation necrosis. As part of an ongoing longitudinal study, an imaging plan had been devised in which a patient with a suspect lesion would undergo multiple scans at a frequency of approximately one scan per week in an attempt to capture the progression of a lesion and the response of the lesion to therapy or therapy modifications. Having recently had an ambiguous PET scan, this patient was chosen to be an appropriate case for implementation of the protocol. The patient signed an informed Internal Review Board approval consent.

Images

Images for this study were acquired using a 3.0 T MR system (Signa 5.x Echospeed; GE Medical Systems, Milwaukee, WI, U.S.A.). The following images were collected: T1-weighted 3D volumes (TR/TE/NEX 400/10/2 ms, slice thickness 3 mm, interslice gap 0, matrix 256 × 192, 24 cm field of view) and proton density (TR/TE/NEX 5,000/18/2, slice thickness 3 mm, interslice gap 0, 256 × 192 matrix, 24 cm field of view). Postcontrast T1-weighted images were acquired immediately following the administration of 20 ml of Gd-DTPA, an MR contrast agent (Magnevist; Berlex Laboratories, Wayne, NJ, U.S.A.). The patient was scanned on 15 occasions at intervals ranging from 2 to 21 days. The scan interval was 7 days in most instances.

Image Processing

All scans were RF corrected to eliminate signal fluctuations due to distortions in the magnetic field of the

FIG. 1. Tracking contrast enhancement volume. The graph illustrates the change in volume of contrast-enhancing tissue across time. Addition of temozolomide to the therapy regimen began on day 45. Note the attenuation of growth rates following the initiation of treatment.
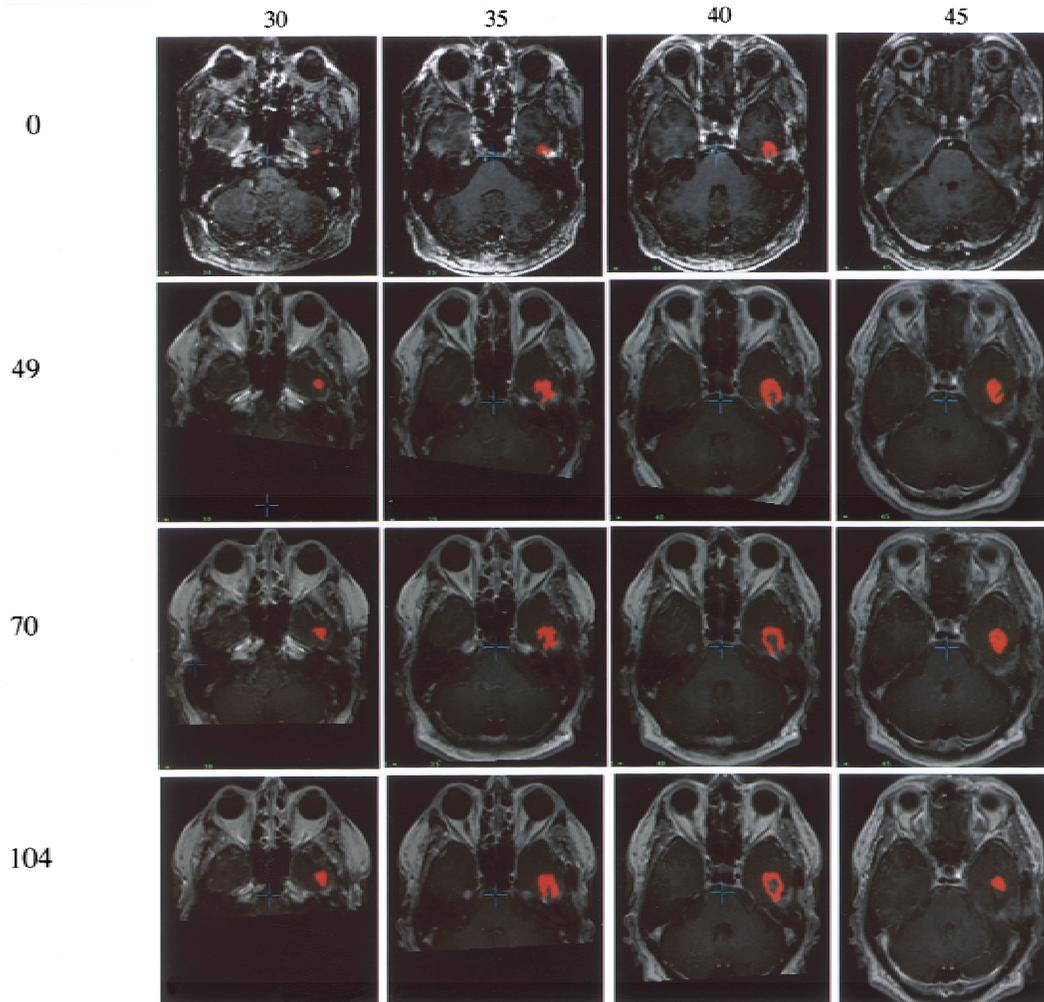
FIG. 2. Slice comparison across time (axial level in mm, Talairach space). This figure illustrates the change in the border of contrast-enhancing tissue across time. As stereotaxic space is maintained, the change at each slice level may be followed. This is useful in distinguishing subtle advances of the border of contrast-enhancing tissue.

scanner (6). SGI 180 MHz (R10000) workstations were used to align and segment the images. Image volumes were manually aligned using six parameter rigid transformation to a population-based average brain data set (7,8) in Talairach stereotaxic space (9). Software developed at UCLA was used for manually assisted image registration. Manual alignment offered better registration of internal anatomically relevant structures than more automated alignment software (10). To perform tissue classification, the following protocol was followed: One hundred sixty tags representing points in white matter, gray matter, CSF, background, tumor, and edema were selected. Segmentation was performed through the use of population-based tissue maps. Population-based tissue maps, containing probabilistic information on tissue location in stereotaxic space, were automatically aligned with scan data, adjusted for herniation effects with nonlinear registration, and used to determine a Gaussian mixture distribution reflecting the intensities of specific tissue classes at each time point in the scan series. Tissue types were differentiated through the use of a nearest-neighbor algorithm, the accuracy of which was confirmed by tagging points in each anatomically relevant region. Tissue maps for tumor were generated and manually adjusted so that class boundaries between tissue types could be better delineated. For the surface-modeling algorithm, the following steps were performed: An operator defined the boundaries of the contrast-enhancing tumor. Traced points were then converted by a surface-modeling algorithm into a tiled parametric mesh model. The algorithm uniformly re-digitized the points at each level in adjacent sections and reconstructed the surface using triangular tiles (11). Volumes were then determined from the 3D mesh models.

RESULTS

The volumes of contrast enhancement were determined and followed (Fig. 1). Initially, the volume more

than tripled over a 34 day period during which time the patient was scanned six times.

In this case, the patient was treated with temozolomide, an imidazotetrazine derivative, which is related to mitozolomide. Temozolomide, a prodrug, degrades in physiological solutions to form the methylating cytotoxic derivative MTIC [5-(3-methyltriazen-1-yl)imidazole-4-carboxamide]. The binding of MTIC to DNA guanine bases is thought to be responsible for the antitumor effect of the drug (12). The patient, already receiving Accutane (100 mg/m^2/day × 21 days, 7 days off), was started on temozolomide (200 mg/m^2/day × 5 days, 23 days off) on day 45. After the administration of temozolomide, the volume increased further, though the rate of increase decreased and a plateau was reached on day 55 (volume = 3.3 cm^3 as determined by the tissue segmentation algorithm; 4.0 cm^3 as determined by the surface-modeling approach). By graphing the volumetric data across time, an alteration in the growth rate of the tumor, as evident by the slope of the graph, is clear (Figs. 1 and 2). The growth rate from the time of the initial scan until the start of therapy (day 10 to 45) was estimated to be 1.5 cm^3/month. The rate of growth decreased somewhat in the 11 days following therapy to 1.4 cm^3/month (day 45 to 56). By the next scanning date, day 63 of the study, growth, as measured by the volume change in contrast enhancement, had plateaued. From this point through the remainder of the study, the volume oscillated around the volume obtained on day 54. Radiologically, the tumor would be described as stable disease. This alteration in the course of tumor growth, as captured by short-interval repeat scanning, illustrates the temporal relationship of the initiation of therapy and the effect of therapy. The change in tumor is clearly captured by the surface-modeling algorithm (Fig. 3). Differential growth rates may be derived from the surface model volumes as well (Fig. 4). Patterns of differential growth allow regions of rapid growth to be segregated from more stable areas. For the growth data to be useful in the planning of surgery or guiding biopsy, stereotaxic space must be maintained across time. The surface-modeling algorithm is able to do this (Fig. 5).

DISCUSSION

To more fully understand tumor changes and provide effective treatments to combat tumor growth, a better definition of tumor on MRI is needed. Histopathologic correlation between biopsy tissue and imaging, as well as a greater understanding of imaging markers both prior to and subsequent to therapy, will aid substantially in achieving this goal. Short-interval scanning also provides a means to achieve this goal: (a) it provides detailed information about the natural progression of tumor growth prior to therapy; (b) it closely follows the temporal sequence of how and when imaging markers re-

Day	0	42	49	104
Volume cm^3	0.8	3.4	3.9	2.5
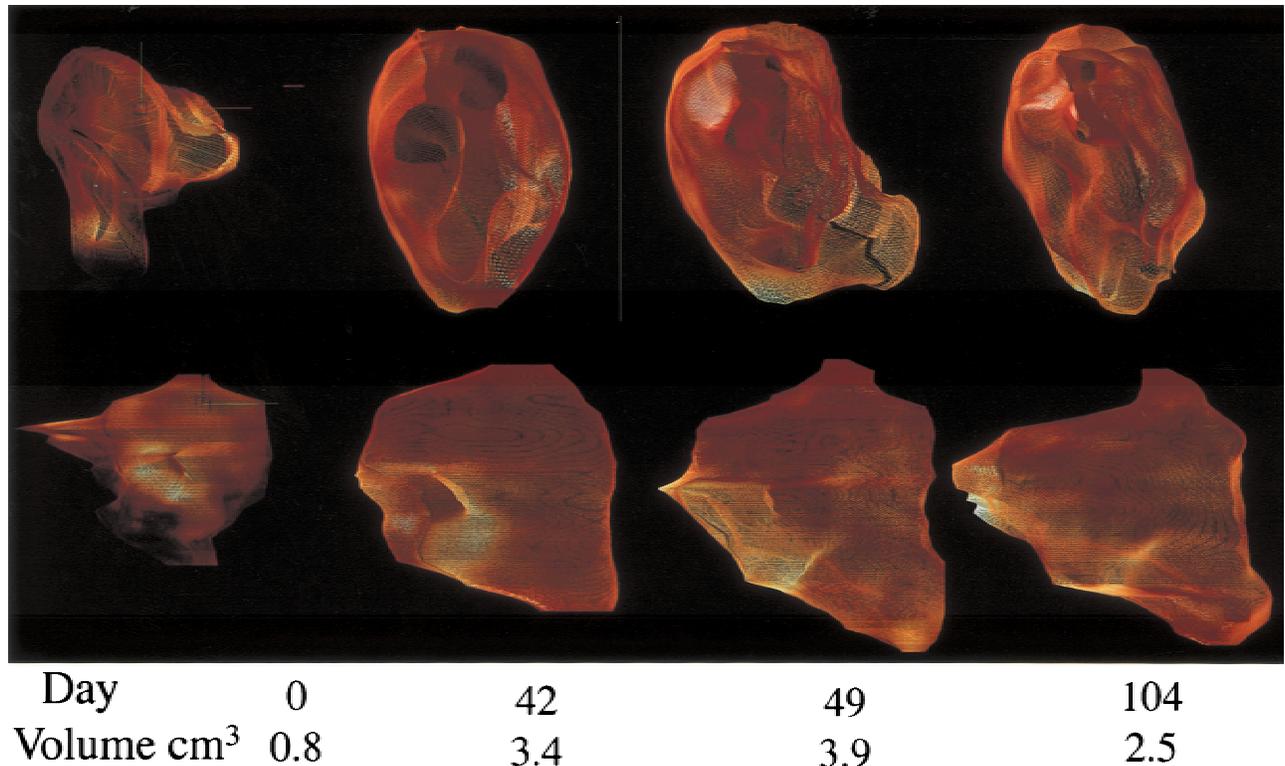
FIG. 3. Surface mesh models across time. The surface-modeling algorithm generates mesh models that, when examined across time, reveal differential growth patterns. This figure illustrates the models as seen from above and from the side. Details of focal change may be determined from the growth patterns derived from the mesh models.
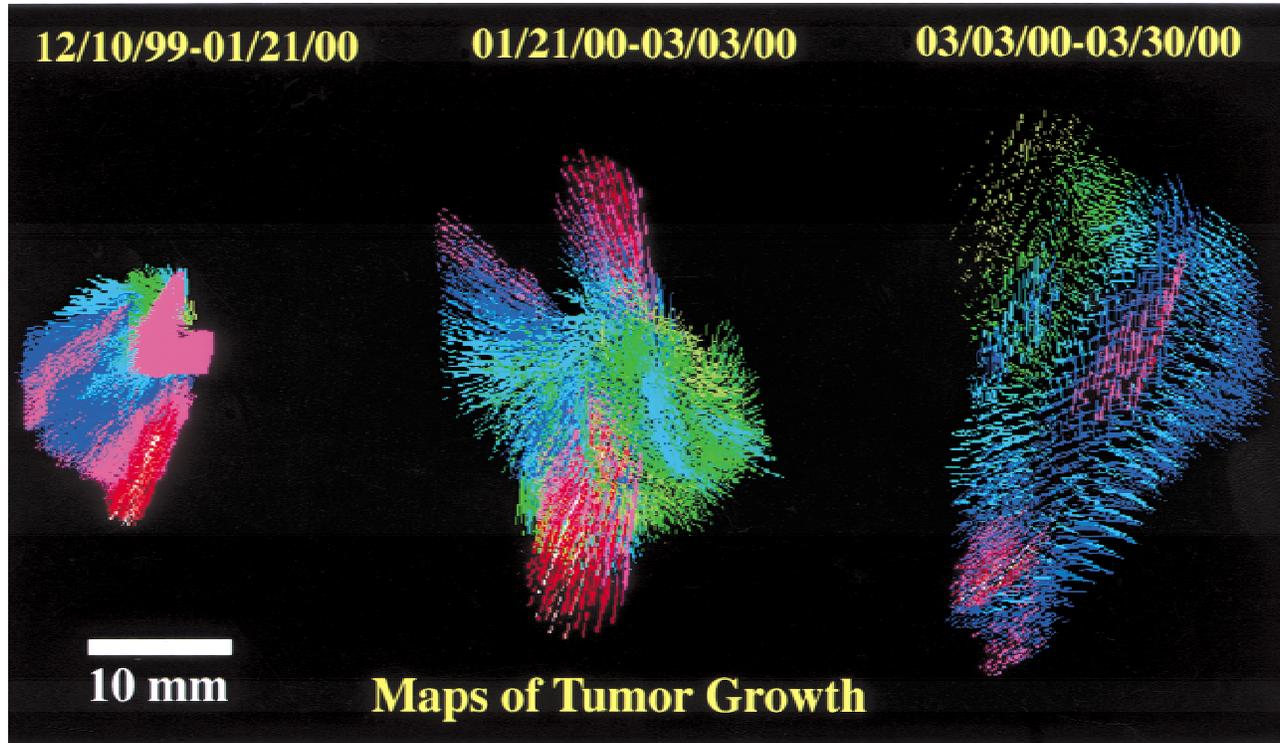
FIG. 4. Vector maps (ref. 4) illustrate both the magnitude and the direction of tumor growth during a time interval. They track change on a point-by-point basis and reveal a heterogeneous growth profile across the tumor surface. The 3D displacement vectors (pink colors: high growth; blue colors: low growth) reveal aggressive growth that is attenuated after change of therapy.

spond once therapy is initiated; and (c) it yields growth rate, a surrogate marker that may be used to judge the efficacy of therapy. In this study, a patient with GBM was followed prior to and subsequent to treatment with temozolomide, revealing modulation in the 3D profile of growth.

This study is novel in terms of the frequency, the number of scans, and the application of tissue segmentation and surface-modeling algorithms to determine response to therapy. Studies, including that of Ross et al. (13), assessing response to therapy, have been performed previously in animal models. Through frequent scanning, we were able to follow the natural progression of the tumor prior to therapy. Subsequent to treatment, an attenuation of growth followed by cessation in growth was observed. Short-interval scanning provided a means to determine the temporal relation of therapy to a marked, observable response.

Despite initial growth in contrast-enhancing volume after therapy, determining growth rate across time clearly showed that therapy was effective. The natural progression of tumor had been altered and growth had ceased. Growth rates may then serve as a surrogate marker for response. The response might not have been appreciated had it not been for the tight interval between scans. An increase in volume, depending on when the scan was taken, might have been interpreted as therapy failure and an effective therapy might then have been discontinued to the detriment of the patient. With the addition of

growth rates to the small arsenal of imaging markers, more data will be available for the evaluation of therapies. In this case study, we demonstrated that the tissue segmentation and surface-modeling algorithms were able to track change through short-interval scanning. Future studies may be designed to accommodate a greater number of patients and include histopathologic correlation from stereotaxically guided biopsy with the imaging results, specifically the results of the surface-modeling algorithm. In the case of this study, the patient's tumor had stabilized, so there was no medical indication to perform stereotaxically guided biopsy.

It is worth noting that contrast enhancement volume is not tumor proper itself. Rather, enhancement represents a breakdown of the blood-brain barrier with subsequent extravasation of contrast enhancement into the surrounding parenchyma. Contrast enhancement may therefore serve as an adjunct marker for tumor volume. It is used partially for this purpose clinically. A method used by the Eastern Cooperative Oncology Group and the Radiation Treatment Group determines response to therapy based on the area of contrast enhancement in a single MR slice (14). In a study by Filipek et al. (5), growth rates, as measured by change in contrast enhancement, were sensitive enough to predict response.

Segmentation

Contrast enhancement volumes were determined independently by two algorithms: tissue classification and
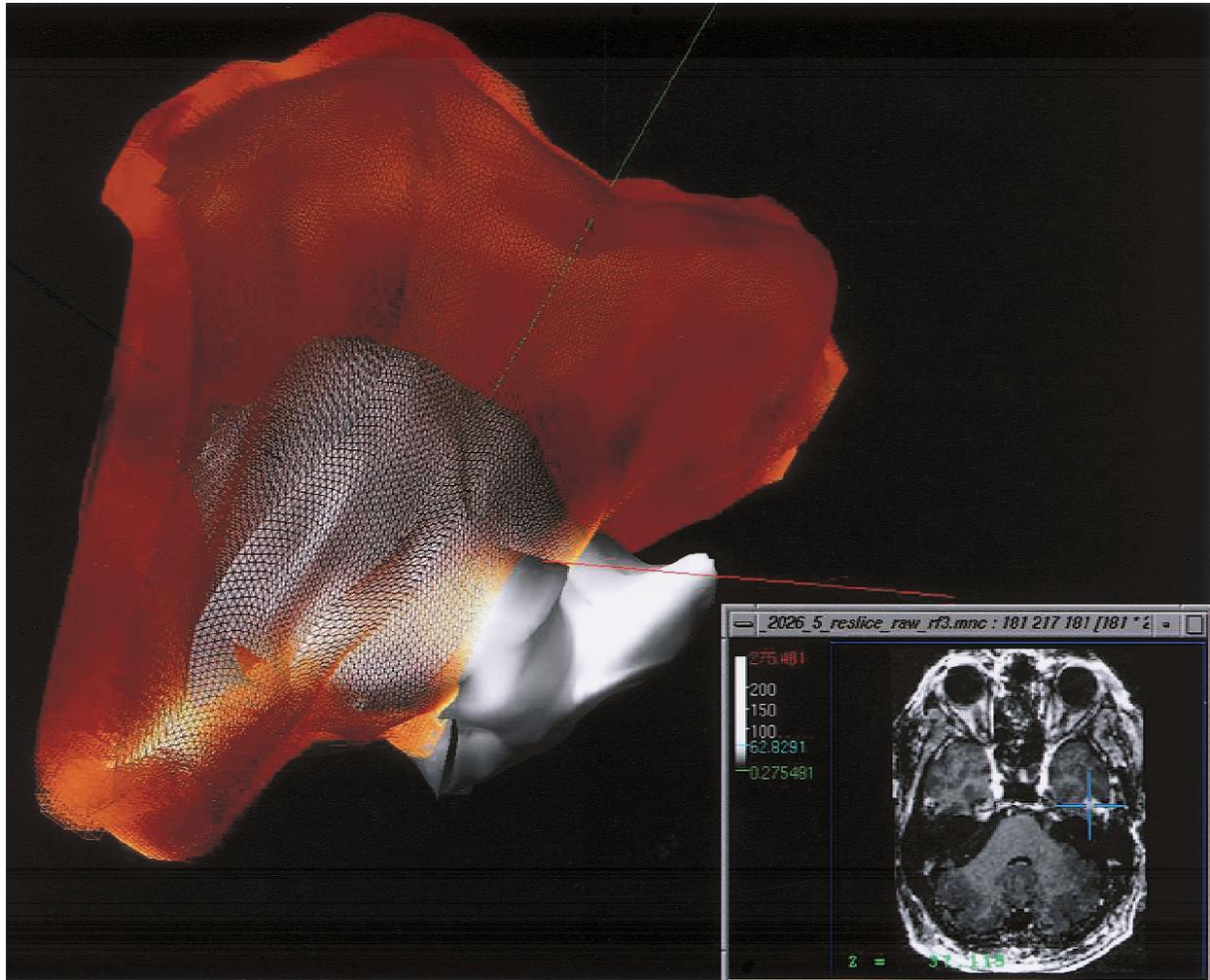
FIG. 5. As the mesh models reveal differential growth and stereotaxic space is maintained, the surface-modeling algorithm may be used to guide biopsy of a specific region of the tumor, for example, the most aggressive region. This may in turn provide information on the genetic heterogeneity of the tumor, which may be used to direct therapy decisions. For example, if a resistance mechanism were found to be present in a particularly aggressive region of the tumor, this information could be used to appropriately direct therapy decisions.

surface modeling (Figs. 3, 5, and 6). Both algorithms have been successfully applied previously to segmentation of brain tissue. The segmentation models generated by the algorithm may be analyzed across time, thereby revealing patterns of differential growth in tumor (Figs. 3 and 4). The segmentation models are generated in such a manner that stereotaxic space is maintained (Fig. 5). This allows for alignment of data from other imaging modalities such as PET and MRS.

Defining surface-to-surface correspondences to model anatomic changes across time is complex. In cases where the same anatomy is present at both time points, a parametric grid, with a specific grid structure, may be overlaid over each surface and correspondences inferred by matching corresponding grid locations across time. To accommodate more complex correspondences between a specific region of one surface and a specific region of another, we previously developed a set of mathematical algorithms that are capable of explicitly matching land-

mark points and curves within surfaces, while also matching the entire surface geometry exactly (15). Although these methods can be used powerfully to match gyral patterns of the cortical surface from one subject or one time point to another (15), in this work we used a simpler correspondence model, based on parametric grids, owing to the difficulty of establishing meaningful boundary correspondences in cases of infiltrative growth. We are currently validating additional methods for mapping boundary change based on deformable surfaces, using anatomic information to constrain the matching of stable and recurrent regions of tumors.

The tissue classification approach is based on a nearest-neighbor algorithm. The nearest neighbor is a robust, well tested algorithm, capable of segmenting tissue into white matter, gray matter, CSF, edema, and tumor, as represented by contrast enhancement (Fig. 6). The algorithm is stable (16–19). It is also one of the quickest algorithms in terms of both operator input and execution
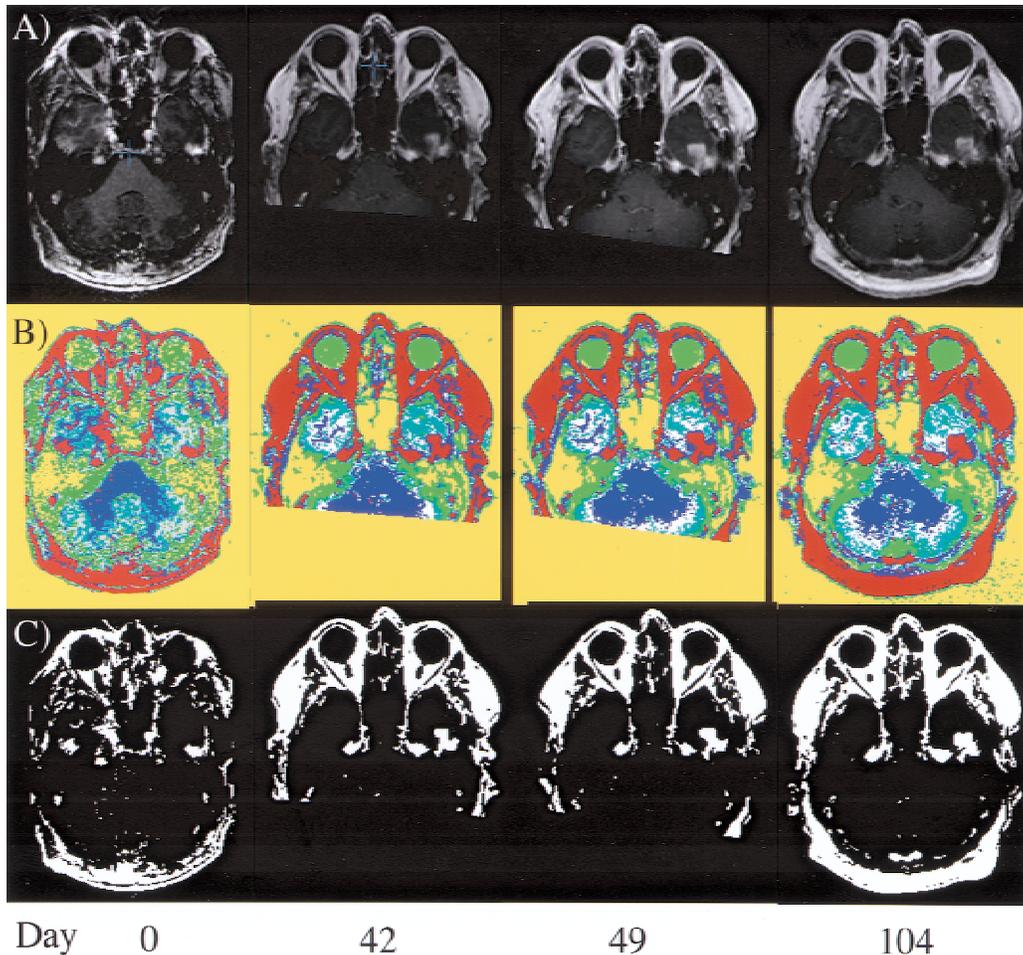
FIG. 6. Nearest-neighbor algorithm tissue classification. Volumetric analysis with the nearest-neighbor tissue classification algorithm is accomplished by generating a tissue segmentation map. From the segmentation map, a binary component map may be generated. In this figure, slices of raw postcontrast T1-weighted MR images (**A**), tissue segmentation maps (**B**), and binary tumor maps (**C**) are shown across time. The algorithm, though not operator-free, reliably generates volumes for contrast-enhancing tissue.

time (16,17). The algorithm detects anatomically relevant structures in cases where more automated algorithms have more difficulty (11,18). These properties may make the nearest-neighbor algorithm well suited for large-scale trials where volume analysis algorithms may provide data on the efficacy of therapy. Further, enhancement volumes as determined by the algorithm are highly correlated with manually defined volumes (3). Recently, Kaus et al. (19) accurately determined the volumes of meningiomas and low-grade gliomas through the application of the nearest-neighbor algorithm.

A surface-modeling algorithm has been used for detecting asymmetry in cortical patterns, for analyzing corpus callosum morphology in schizophrenic patients (20), and in mapping growth rates of the corpus callosum in children (18). Contrast enhancement volumes as determined through the use of the surface-modeling algorithm are highly correlated with enhancement volumes determined manually (21). Capable of tracking change on a point-by-point basis, the surface-modeling algorithm is able to generate highly detailed maps of focal change in enhancement volume across time (Fig. 2). The detailed nature of the maps and the fact that the spatial relationship is stereotaxically maintained make the surface-modeling algorithm well suited for a particular purpose: taking a biopsy from a specific tumor region. Underlying differential tumor growth may relate to genetic or cellular heterogeneity of the tumor. Knowledge of the genetic composition of a tumor would provide an additional basis for therapy decisions by the clinician. Specifically, a genetic analysis of an aggressive region of tumor showing the presence of a drug resistance mechanism would allow the clinician to make appropriate therapy choices.

As good as the surface-modeling algorithm is at estimating change in tumor tissue and as helpful as stereotaxically guided biopsy may potentially be in determining the genetic heterogeneity of tumor tissue, any discussion on tumor growth would be incomplete without recognizing that there are multiple factors that affect tumor growth. Biomechanical factors such as the growth of tumor in the area of least resistance have been shown to be important determinants in the spread of tumor tissue

(22). Wasserman et al. (23) developed a comprehensive model for patient-specific in vivo tumor growth. This model incorporates mechanical influences and important factors such as cell adhesiveness, oxygen distribution, production of lytic enzymes, pH, and immune system responses in determining tumor growth. As tumor growth is multifactorial, and given that growth may preferentially occur into the area of least resistance rather than from the most malignant region, it is difficult to draw the conclusion that the area of greatest tumor growth is the most malignant. Nonetheless, important information about the genetic nature of the tumor may be obtained through stereotaxically guided biopsy, and this information may aid the clinician in choosing a course of therapy.

CONCLUSION

Short-interval scanning reveals natural tumor progression prior to therapy. After therapy, short-interval scanning clearly demonstrated cessation of growth in this case. Tracking tumor growth clearly showed the effect of therapy. As such, growth rates may serve as a surrogate end-point for determination of therapy response. The volumetric measurements, forming the basis on which growth were determined, were achieved by independently applying a tissue segmentation algorithm and a surface-modeling algorithm. Finally, short-interval scanning may provide a better understanding of imaging markers, which may prove useful in evaluating new therapies.

REFERENCES

1. Djulbegovic B, Sullivan D, *Decision Making in Oncology: Evidence Based Management*. Philadelphia: Churchill Livingstone, 1997:353–7.
2. Imperato JP, Paleologos NA, Vick NA. Effects of treatment on long-term survivors with malignant astrocytomas. *Ann Neurol* 1990;28:818–22.
3. Mega MS, Chen SS, Thompson PM, et al. Mapping histology to metabolism: coregistration of stained whole brain sections to premortem PET using 3D cryomacrotome reconstruction as a reference. *Neuroimage* 1997;5:147–153.
4. Thompson PM, Mega MS, Toga AW. Disease-specific brain atlases. In: Toga AW, Mazziotta JC, Frackowiak RSJ, eds. *Brain Mapping: The Disorders*. San Diego, CA: Academic Press, 2000:131–77.
5. Filipek P, Kennedy D, Caviness V. Volumetric analyses of central nervous system neoplasm based on MRI. *Pediatr Neurol* 1991;7:347–51.
6. Sled J, Zijdenbos A, Evans A. A nonparametric method of automatic correction of intensity of nonuniformity in the MRI data. *IEEE Trans Med Imag* 1998;17:87–97.
7. Evans A, Collins D, Neelin P, et al. Three-dimensional correlative imaging: applications in human brain mapping. In: *Functional Neuroimaging: Technical Foundations*. San Diego: Academic Press, 1994:145–62.
8. Mazziotta JC, Toga AW, Evans AC, et al. A probabilistic atlas of the human brain: theory and rationale for its for development. *Neuroimage* 1995;2:89–101.
9. Talairach J, Tournoux P. *Co-Planar Stereotaxic Atlas of Human Brain*. New York: Thieme, 1988.
10. Woods R, Mazziotta J, Cherry S. MRI-PET registration with automated algorithm. *J Comput Assist Tomogr* 1993:536–46.
11. Thompson PM, Schwartz C, Toga AW. High-resolution random mesh algorithms for creating a probabilistic atlas of the human brain. *Neuroimage* 1996;3:19–34.
12. Meikle SR, Matthews JC, Brock CS, et al. Pharmacokinetic assessment of novel anti-cancer drugs using spectral analysis and positron emission tomography: a feasibility study. *Cancer Chemother Pharmacol* 1998;42:183–93.
13. Ross BD, Zhao YJ, Neal ER, et al. Contributions of cell kill and post-treatment tumor growth rates to the repopulation of intracerebral 9L tumors after chemotherapy. *Proc Natl Acad Sci USA* 1998;95:7012–7.
14. Clarke LP, Velthuizen RP, Clark M, et al. MRI measurement of brain tumor response: comparison of visual metric and automatic segmentation. *Magn Res Imag* 1998;16:271–9.
15. Thompson PM, Woods RP, Mega MS, et al. Mathematical/computational challenges in creating deformable and probabilistic atlases of the human brain. *Hum Brain Map* 2000;9:81–92.
16. Bezdek J, Hall L, Clarke L. Review of MR image segmentation techniques using pattern recognition. *Med Phys* 1993;20:1033–47.
17. Clarke LP, Velthuizen RP, Phuphanich S, et al. MRI: stability of three supervised segmentation techniques. *Magn Res Imag* 1995;11:95–106.
18. Thompson PM, Giedd JN, Woods RP, et al. Growth patterns in developing human brain detected using continuum-mechanical tensor mapping. *Nature* 2000;404:190–3.
19. Kaus M, Warfield S, Nabavi A, et al. Segmentation of meningiomas and low grade gliomas in MRI. *Proceedings of Second International Conference on Medical Image Computing and Computer-Assisted Interventions (MICCAI)*, Cambridge, U.K., 1999;1:1–10.
20. Narr KL, Thompson PM, Sharma T, et al. 3D morphology of the corpus callosum in schizophrenia. *Cereb Cortex* 2000;10:40–9.
21. Haney S, Thompson PM, Alger JR, et al. Mapping dynamic patterns of tumor growth in patients with glioblastoma multiforme [Abstract]. Proc Society for Neuroscience, Miami, FL, 1999.
22. Eaves G. The invasive growth of malignant tumors as a purely mechanical process. *J Pathol* 1973;109:233–7.
23. Wasserman R, Acharya R, Sibata C, et al. A patient-specific in vivo tumor model. *Math Biosci* 1996;136:111–40.